9668 *Biochemistry* **2009,** *48,* 9668–9676
DOI: 10.1021/bi901149t

BIOCHEMISTRY
including biophysical chemistry & molecular biology
Article

Unique Ligand Binding Patterns between Estrogen Receptor α and β Revealed by Hydrogen−Deuterium Exchange†

Susie Y. Dai,[‡,⊥] Thomas P. Burris,[∥,#] Jeffrey A. Dodge,[∥] Chahrzad Montrose-Rafizadeh,[∥] Yong Wang,[∥] Bruce D. Pascal,[§] Michael J. Chalmers,[‡,§] and Patrick R. Griffin*[,‡,§]

[‡]*Department of Molecular Therapeutics and* [§]*The Scripps Research Molecular Screening Center, The Scripps Research Institute, Scripps Florida, Jupiter, Florida 33458, and* [∥]*Lilly Research Laboratories, Eli Lilly and Company, Indianapolis, Indiana 46285* [⊥]*Present address: Office of the Texas State Chemist, Department of Veterinary Pathobiology, Texas A&M University, College Station, TX 77843.* [#]*Present address: Department of Molecular Therapeutics, The Scripps Research Institute, Jupiter, FL 33458.*

Received July 7, 2009; Revised Manuscript Received September 9, 2009

ABSTRACT: Here we present the use of hydrogen−deuterium exchange (HDX) mass spectrometry in analyzing the estrogen receptor β ligand binding domain (ERβ LBD) in the absence and presence of a variety of chemical compounds with different binding modes and pharmacological properties. Previously, we reported the use of HDX as a method for predicting the tissue selectivity of ERα ligands. HDX profiles of ERα LBD in complex with ligand could differentiate compounds of the same chemotype. In contrast, similar analysis of ERβ LBD showed correlation to the compound chemical structures but little correlation with compound tissue selectivity. The different HDX patterns observed for ERβ LBD when compared to those for ERα LBD bound to the same chemical compounds serve as an indication that ERβ LBD undergoes a different structural response to the same ligand when compared to ERα LBD. The conformational dynamics revealed by HDX for ERβ LBD together with those for ERα LBD shed light on ER ligand interactions and offer new structural insights. The compound-specific perturbations in HDX kinetics observed for each of the two isoforms should aid the development of subtype-selective ER ligands.

Estrogen receptors (ERα and ERβ) belong to the nuclear receptor superfamily functioning as ligand-dependent transcription factors and play important roles in a variety of processes, including regulation of the reproductive and cardiovascular systems, bone density, cognition, and inflammation (*1*−*4*). Although the two isoforms share common domain structure with 94% identical amino acids in their DNA binding domains (DBDs) and 53% identical amino acids in the ligand binding domains (LBDs)[1] (*1*), ERα and ERβ have different tissue expression profiles and exhibit distinct biological functions in several disease phenotypes (*4*−*8*). Not surprisingly, both ER isoforms bind a wide spectrum of natural and synthetic ligands, and recent efforts have focused on the development of isoform-selective ER modulators for improved therapies for prostatic diseases, inflammation, and arthritis (*8*, *9*). Since many of the compounds developed to target ERα also bind to ERβ with comparable affinity and potency, the study of the receptor−ligand interaction for each isoform is important for understanding how those ligands regulate ER functions from a structural basis.

Previous crystallographic analyses of both ERs revealed a canonical fold for the ER ligand binding domain (*10*−*12*). In these X-ray structures, 12 helices are arranged in a three-layer sandwich topology and the receptors hold a hydrophobic cavity for hormone binding. It is believed that agonist or antagonist binding induces a distinct conformation change in the receptor that initiates activation or suppression of responsive genes as determined by the preferential association or dissociation of coactivator and corepressor proteins. Classic ER binding models were validated by the different ER−ligand complex structures in which ligands reside in the steroid binding site and interact with the ER LBD to modulate the position of helix 12 in distinct positions either favoring or disrupting coactivator binding (*10*). The cognate steroid binding sites of the two ER isoforms are nearly identical with only two amino acid residues being different (*11*). Recently, both computational and experimental studies suggested the possibility of other ligand binding sites within the ER LBD, although the putative secondary binding sites were distinct from each other in these two studies (*13*, *14*). Although X-ray studies of the binding modes of many compounds in complex with two isoforms have greatly improved our understanding of the interactions between ER and ligand, these data are not enough to explain the isoform and tissue selectivity of many ER ligands.

HDX mass spectrometry has been used to evaluate the mode of binding of ligands to nuclear receptors (*15*−*19*). We have previously described the structure dynamics of ERα in the presence of a variety of natural or synthetic compounds representing agonism, antagonism, or selective agonism with tissue specificity (*20*). Differential HDX analysis of the LBD of ERα in complex with various ligands revealed that alterations in structural dynamics can be related to a compound's pharmacological

†M.J.C. and P.R.G. acknowledge funding from the National Institutes of Health [U54-MH074404 (principal investigator, H. Rosen) and GM084041].

*To whom correspondence should be addressed: The Scripps Research Institute, Scripps Florida, 130 Scripps Way, Jupiter, FL 33458. Phone: (561) 228-2200. Fax: (561) 228-3081. E-mail: pgriffin@scripps.edu.

[1]Abbreviations: HDX, hydrogen−deuterium exchange; ER, estrogen receptor; LBD, ligand binding domain; E2, estradiol; DES, diethylstilbestrol; PDB, Protein Data Bank.

 Published on Web 09/09/2009

properties and thus provide a novel approach to probing selective estrogen receptor modulators (SERMs). Here we compare the HDX characteristics of the LBD of ERβ with ERα in complex with the same set of ligands. At the same time, we have measured the binding affinity of the same array of compounds for both receptors. Generally, all the ligands bind tightly to both receptors with the binding affinity in the low nanomolar range, with some showing preference for either receptor. In addition, the HDX profiles of both ERα and ERβ in complex with genistein were compared. Genistein is an isoflavonoid phytoestrogen ERβ-selective ligand. The binding of genistein to ERβ is approximately 10-folder tighter than that to ERα according to previous research (*21*). Interestingly, distinct HDX patterns were observed for ERβ and ERα upon binding of each ligand in the compound set, suggesting a distinct function for ERβ in estrogen action regulation. HDX data for ERβ, together with the published HDX data of ERα, provide unique insight into the ligand-dependent activation of the two ERs.

MATERIALS AND METHODS

Protein and Reagents for HDX Analysis. The ERβ LBD (amino acids 257−502) was overexpressed as an N-terminally His_6-tagged protein in BL21(DE3) cells by using vector pET19 (Novagen), and the purified protein was provided by PanVera (Madison, WI). All compounds were from Lilly Research Laboratories except raloxifene and genistein which were from Sigma (St. Louis, MO). For HDX analysis, ERβ LBD was incubated with compound for 1 h at a ratio of 1:10. The protein concentration was 12 μM in the deuterium incubation buffer, which is the same condition used for the ERα−ligand study we performed earlier. The ERα LBD−genistein experiment followed the conditions that have been reported previously (*20*) at a receptor:ligand ratio of 1:10.

HDX Analysis. HDX experiments were conducted with a LEAP Technologies Twin HTS PAL liquid handling robot interfaced with a Thermo Finnigan LTQ mass spectrometer (Thermo Electron Corp., San Jose, CA). For a complete experimental description, see ref *17*. Briefly, the protein−ligand complex was diluted into a D_2O exchange buffer and subjected to HDX for 1, 30, 60, 900, and 4200 s. HDX experiments were performed at 4 °C by dilution of 4 μL of the ER LBD solution with 16 μL of D_2O buffer containing 20 mM Tris-HCl, 100 mM KCl, and 1 mM DTT (pD 7.9). After the incubation in D_2O at an aforementioned fixed hydrogen−deuterium exchange time, the exchange reaction was quenched with 2 M urea containing 1% TFA and the mixture passed over an in-house packed pepsin column (2 mm × 2 cm) which was kept at 2 °C. The digested ER LBD peptides were then eluted through a 2.1 mm × 1 cm C_8 trap cartridge (Eclipse XDB-C8, Agilent, Santa Clara, CA) and desalted. The digestion and desalting take a total of 2.5 min. Peptides were then eluted across a 2.1 mm × 5 cm C_{18} column (Thermo Scientific, Waltham, MA) with a linear gradient from 2 to 50% B over 10 min (solvent A, 0.3% formic acid in water; solvent B, 0.3% formic acid with 80% acetonitrile and 20% water; flow rate of 200 μL/min) (*22*). Mass spectrometric analyses were conducted with a capillary temperature of 225 °C.

Peptide Identification and HDX Data Processing. Product ion spectra were acquired in a data-dependent MS/MS mode. The precursor ion survey scan was performed, and the five most abundant ions were selected for product ion analysis. MS/MS *.raw data were searched against the database containing ER using SEQUEST (Bioworks, Thermo Finnigan). At the same time, the MS/MS *.raw data files were converted to *.dta and *.mgf files and submitted to Mascot (Matrix Science, London, U.K.) for searching against a database containing ER. All peptide ion assignments were inspected manually.

The weighted average m/z values of each peptide ion isotopic cluster were calculated with the Web-based software known as "Deuterator" (*23*). The deuteration level was calculated on the basis of the following equation, and the corrections for back-exchange were made using 70% deuterium recovery and accounting for 80% deuterium content in the on-exchange buffer:

$$\text{deuteration level (\%)} = \frac{m/z(\text{P}) - m/z(\text{N})}{m/z(\text{F}) - m/z(\text{N})} \times 100$$

where m/z(P), m/z(N), and m/z(F) are the centroid value of the partially deuterated peptide, the nondeuterated peptide, and the fully deuterated peptide, respectively (*24*).

ER Binding Assay. The competition binding assay was performed in a buffer containing 50 mM Hepes (pH 7.5), 1.5 mM EDTA, 150 mM NaCl, 10% glycerol, 1 mg/mL ovalbumin, and 5 mM DTT, using 0.025 μCi of [^{3}H]estradiol (NEN catalog no. NET517 at 118 Ci/mmol, 1.5 nM E2) (NEN/PerkinElmer, Boston, MA) or 10 ng of ERα or ERβ per well. Nonspecific binding was determined in the presence of 1 μM 17-β-estradiol (E2). The binding reaction mixture was incubated for 4 h at room temperature, and then a cold DCC buffer was added to each reaction mixture [the DCC buffer contains, per 50 mL of assay buffer, 0.75 g of charcoal (Sigma) and 0.25 g of dextran (Pharmacia, Uppsala, Sweden)]. Plates were mixed for 8 min on an orbital shaker at 4 °C and then centrifuged at 3000 rpm and 4 °C for 10 min. An aliquot of the mix was added to Wallac Optiphase "Hisafe 3" scintillation fluid, incubated for 5 h, and read in a Wallac Microbeta counter. The K_d for [^{3}H]estradiol was determined by saturation binding for ERα or ERβ receptors. The IC_{50} values for compounds were converted to K_i values using the Cheng−Prusoff equation.

Cell-Based Functional Assay. Human embryonic kidney HEK293 cells were cultured in DMEM/Ham F12 (3:1) medium without phenol red in the presence of 50 μg/mL gentamicin and 10% heat-inactivated FBS (Gibco BRL, Rockville, MD). One day prior to the experiment, 3×10^6 cells were seeded onto DMEM/Ham F12 (3:1) medium without phenol red in the presence of 10% charcoal-stripped heat-inactivated FBS (Gibco BRL) and 50 μg/mL gentamicin in a T225 tissue culture flask. Cells were transfected with 250 μL of Fugene (Roche Biologicals, Mannheim, Germany), 100 μg of plasmid-containing ERE response element upstream of a minimal thymidine kinase promoter-driven luciferase gene, and 10 μg of expression vector for hERβ receptor-driven viral CMV promoter (pCMVhERβ expression plasmid). After 5 h, cells were transferred to a 96-well tissue culture dish and the medium was replaced with DMEM/Ham F12 (3:1) medium without phenol red in the presence of 10% charcoal-stripped heat-inactivated FBS (Gibco BRL) without gentamicin. Cells were treated with compounds at different concentrations from 10 μM to 0.3 nM in 10-point concentration dilutions. Twenty-four hours later, cells were harvested and assays for luciferase activity were conducted. The activity was measured as relative light units, and the EC_{50} for ERβ is calculated after fitting the data to a four-parameter curve fit. The percent stimulation was calculated versus the DES maximum response.

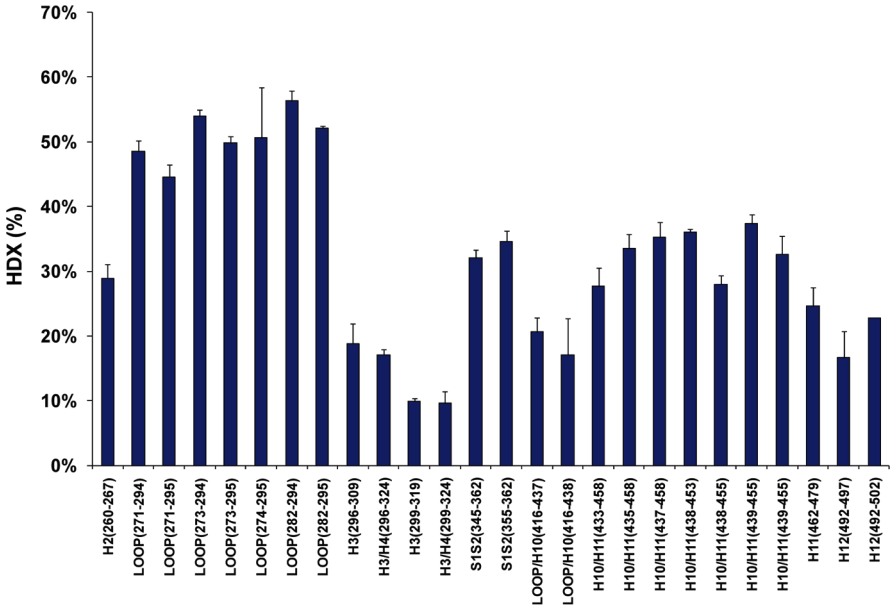

FIGURE 1: HDX percentage of apo ERβ LBD with respect to the secondary structures. The HDX percentage from helix 2 to helix 12 was plotted vs the secondary structures that have peptides available for HDX analysis. The percentage is the averaged value of five HDX experiments with different exchange times (1, 30, 60, 900, and 4200 s). The standard deviation of three independent measurements is showed with an error bar.

RESULTS

HDX Analysis of ERβ LBD. Exchange kinetics for 26 different regions covering 60% of the sequence of the receptor LBD were measured. Figure 1 shows the HDX analysis of the apo ERβ LBD with secondary structure alignment. The percent HDX exchange displayed in Figure 1 is the average of five HDX on-exchange experiments for apo ERβ LBD (exchange times of 1, 30, 60, 900, and 4200 s). In the HDX experiment, none of the peptides analyzed exhibited bimodal deuterium incorporation. In other words, there was no coexistence of deuterated and non-deuterated species, namely, the so-called EX1 exchange regime (*25*). Each on-exchange time point was measured in triplicate, and the standard deviation of the average measurement is shown (*17*).

Comprehensive differential HDX analyses were then performed for the 12 ERβ LBD−ligand complexes. The chemical structures are presented in Figure 2, and the results are summarized in Table 1. The values in Table 1 represent the average differences in deuterium incorporation percentages for the five on-exchange time points for triplicate experiments (1, 30, 60, 900, and 4200 s). A negative percentage represents an increase in the level of protection to exchange in that region of the receptor in the presence of ligand, which indicates the region has been protected when bound with ligand. It is clear that different regions of ERβ LBD present different degrees of protection when binding with the ligand and the same region of ERβ LBD presents a different degree of protection when binding with different ligands. To compare ligand-induced HDX dynamic changes on ERβ LBD, a histogram (Figure 3A) was made with respect to HDX protection (relative HDX exchange in the presence and absence of the ligand) and ER secondary structures. The three compounds plotted are 4-hydroxytamoxifen, estradiol, and genistein. In Figure 3B, the same comparison was made for ERα LBD with or without 4-hydroxytamoxifen, and estradiol from our previous data (*20*), and the addition of the new data from the analysis of ERα LBD with or without genistein. The percentages of HDX exchange protection for both receptors are plotted versus the secondary structures in Figure 3A,B.

Figure S1 of the Supporting Information shows the underlying percent deuterium incorporation (%D) versus log time plots for three regions of ERβ LBD (amino acids 282−294, 492−502, and 355−362) in the presence and absence of estradiol and 4-hydroxytamoxifen. The deuterium incorporation versus log time plots were typical of all peptides measured in this study. ERβ LBD exhibited differential HDX protection in a ligand-dependent and region-specific manner. For example, the β-sheet 1−β-sheet 2 region (amino acids 355−362) was one region that demonstrated the most statistically significant ($p < 0.001$) differential HDX (i.e., ~20% protection to exchange for 4-hydroxytamoxifen) depending on ligand (Figure S1C,F of the Supporting Information). Other regions of the binding pocket, such as helix 12 (Figure S1B,E of the Supporting Information), in the time frame tested have no observable protection to exchange following binding of the ligands studied here, an interesting observation that is consistent with our ERα LBD data. Interestingly, the phytoestrogen genistein shows an HDX profile that does not resemble those of any of the agonists, or SERMs, and provides minimal stabilization to exchange for the ERβ LBD.

Comparison of HDX Data with the Atomic-Resolution Structure. The data from HDX analysis (Table 1) were overlaid onto the X-ray structures of the ERβ LBD−4-hydroxytamoxifen complex. There are three HDX profiles overlaid, which include those of the ERβ LBD−E2 (Figure 4A, HDX data for the ERβ LBD−E2 complex are overlaid on the crystal structure for the ERβ LBD−4-hydroxytamoxifen complex, PDB entry 2FSZ), ERβ LBD−4-hydroxytamoxifen (Figure 4B, PDB entry 2FSZ), and ERβ LBD−genistein (Figure 4C, PDB entry 1QKM) complexes. In the ERβ LBD−4-hydroxytamoxifen complex, the β-sheet 1−β-sheet 2 region (amino acids 355−362) demonstrated the greatest degree of stabilization, which is consistent with data for the ERα LBD (*20*). Note that F356 supplies an aromatic π-edge−face interaction with the hydroxyaryl group that is a ubiquitous feature of nonsteroidal ER ligands (*14*). This very important interaction is nearly at a 180° angle from the trialkyl amine substituents that characterize SERM structures. Further studies such as mutagenesis of F356 (e.g., F356A)

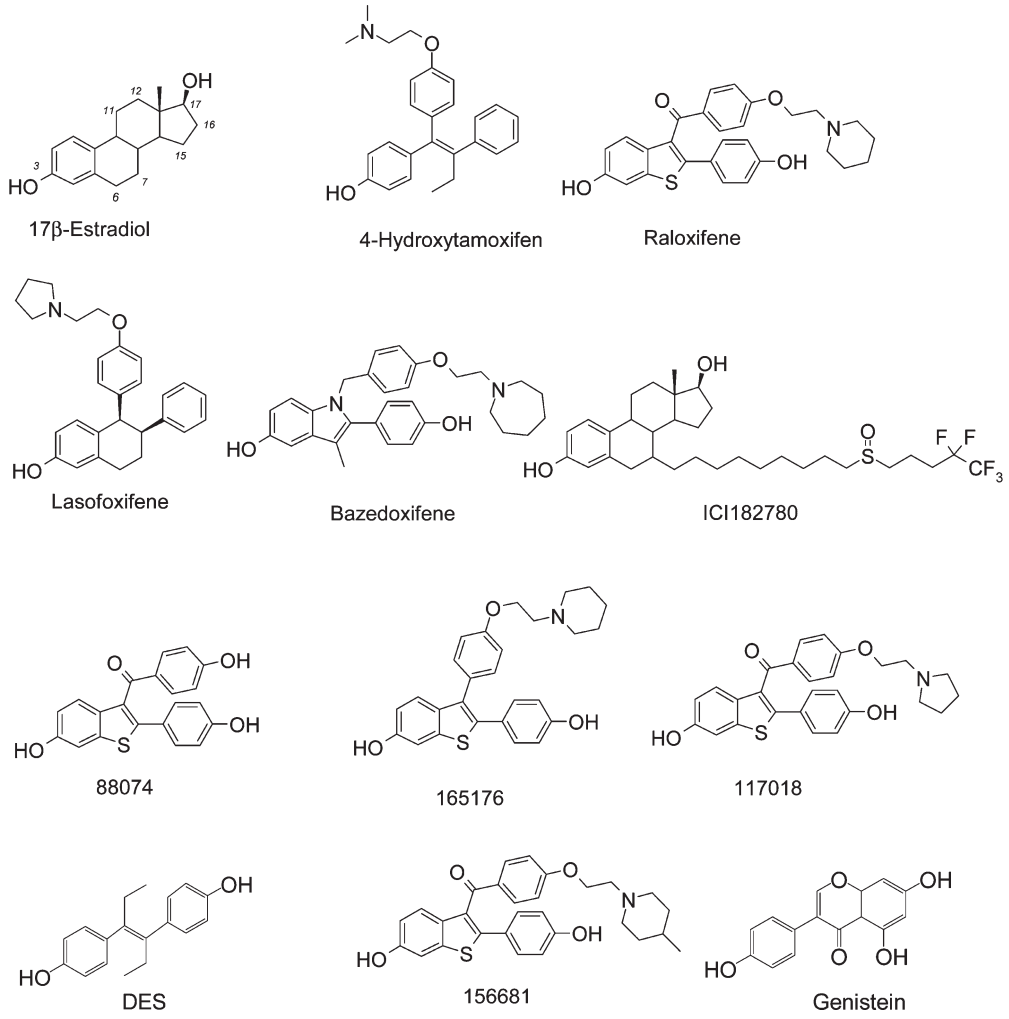

FIGURE 2: Chemical structures of 12 ER ligands.

coupled with HDX analysis of the mutant protein will help in the investigation of the role of F356. However, these studies are beyond the scope of our current study. Helix 4, which covers the second binding site of 4-hydroxytamoxifen residing in the coactivator binding groove, was also stabilized. However, the corresponding peptide spanning this same region in the ERα LBD−4-hydroxytamoxifen complex was not detected with a sufficient signal-to-noise ratio (S/N); therefore, a direct comparison is not available. The helix 5 region was detected in the ERα LBD experiments but showed no protection to exchange.

Statistical Analysis of the Differential HDX Data. In a manner similar to our HDX fingerprint analysis of ERα, a cluster analysis was performed on the 12 ER ligands in the study for which the pharmacological properties are well characterized (*20*). Cluster analysis was performed for 12 compounds with MultiExperiment Viewer (TM4, version 4.0) (*26*). Different cluster methods, including average linkage, complete linkage, and single-linkage cluster, were used, and all rendered similar results. As shown in Figure 5, two major clusters (A and B) were observed. In addition, a unique HDX profile was observed for genistein. Cluster A includes compounds ICI18278, 4-hydroxytamoxifen, DES, lasofoxifene, and bazedoxifene, while cluster B includes 17β-estradiol, raloxifene, and the four benzothiophenes (LY88074, LY165176, LY156681, and LY117018). We found that the ligands in cluster A induced a greater overall degree of protection to exchange within the receptor−ligand complex. The β-sheet 1−β-sheet 2 region experienced the most significant protection to HDX, a pattern consistent across both clusters. Furthermore, ligands in cluster A exhibit a greater degree of protection to exchange in the H10−H11 region than ligands from cluster B. Across both clusters, a rank order of β-sheet 1−β-sheet 2 region > H10−H11 > loop region is observed for those areas with >5% protection. Interestingly, genistein represented a unique HDX profile which may suggest a novel mechanism of interaction with the receptor. Genistein is by far the smallest ligand in the set with a water accessible molecular volume of 828 Å^3 compared to a volume for estradiol of 923 Å^3.

HDX Dynamics and Cellular Activity. To investigate the relationship between HDX and intrinsic cellular function, we evaluated the activity of a subset of ER ligands to assess whether ligand-induced protection to exchange resulted in differences in their intrinsic pharmacological properties at ERβ. Ligands were evaluated for their ability to act as agonists or antagonists of estrogen in HEK293 cells cotransfected with human full-length ERβ. As shown at the bottom of Table 1, 17β-estradiol and DES are potent agonists with EC_{50} values of 0.12 and 0.14 nM, respectively, while ICI is an antagonist with an IC_{50} of 12 nM. For the benzothiophenes, LY88074 is an agonist (EC_{50} = 232 nM) with no antagonist activity (antagonist activity defined as EC_{50} > 10 μM), while LY156681, LY165176, and LY117108 are ERβ antagonists with no agonist activity (EC_{50} > 10 μM). Thus, compounds with similar HDX profiles, such as DES and

Table 1: Average Differences in Deuterium Levels of Apo ERβ LBD in the Presence of Different Ligands with ER Binding Affinity Data and ERβ Agonist/Antagonist Activity[a]

Structure	AA#	End	Estradiol	4-hydroxy tamoxifen	Ralo-xifene	DES	ICI	Lasodo-xifene	Bazedo-xifene	88074	156681	165176	117018	Genistein
H2	260	267	-9%	-12%	-8%	-11%	-10%	-11%	-11%	-7%	-5%	-6%	-6%	-2%
LOOP	271	294	-6%	-8%	-7%	-10%	-9%	-11%	-7%	-7%	-7%	-9%	-7%	-2%
LOOP	271	295	-7%	-11%	-7%	-10%	-10%	-11%	-7%	-8%	-12%	-8%	-7%	-3%
LOOP	273	294	-9%	-12%	-9%	-12%	-11%	-12%	-6%	-9%	-7%	-15%	-8%	-5%
LOOP	273	295	-6%	-11%	-7%	-10%	-10%	-9%	-6%	-7%	-7%	-9%	-7%	-7%
LOOP	274	295	-8%	-12%	-8%	-10%	-11%	-12%	-7%	-8%	-8%	-10%	-8%	-5%
LOOP	282	294	-7%	-10%	-6%	-8%	-9%	-9%	-4%	-7%	-7%	-9%	-7%	-6%
LOOP	282	295	-6%	-11%	-7%	-10%	-10%	-9%	-5%	-7%	-7%	-9%	-8%	*
H3	296	309	-12%	-13%	-10%	-17%	-14%	-16%	-16%	-15%	-9%	-10%	-7%	-8%
H3/H4	296	324	-5%	-9%	-7%	-12%	-10%	-11%	-11%	-8%	-6%	-6%	-5%	-4%
H3	299	319	-8%	-6%	-6%	-9%	-7%	-8%	-8%	-5%	-4%	-4%	-4%	-1%
H3/H4	299	324	-6%	-5%	-3%	-6%	-5%	-6%	-5%	-5%	-2%	-3%	-3%	-2%
S1S2	345	362	-13%	-18%	-14%	-19%	-17%	-19%	-19%	-14%	-14%	-12%	-10%	-3%
S1S2	355	362	-16%	-22%	-16%	-23%	-21%	-24%	-21%	-16%	-12%	-14%	-11%	-5%
LOOP/H10	416	437	-3%	-5%	-4%	-6%	-4%	-6%	-5%	-5%	-3%	-3%	-3%	-2%
LOOP/H10	416	438	-3%	-5%	-3%	-7%	-6%	-7%	-7%	-5%	-3%	-4%	-3%	-3%
H10/H11	433	458	-8%	-11%	-7%	-12%	-10%	-12%	-9%	-9%	-6%	-6%	-5%	-2%
H10/H11	435	458	-9%	-11%	-8%	-12%	-11%	-14%	-13%	-9%	-7%	-8%	-6%	-2%
H10/H11	437	458	-8%	-16%	-8%	-16%	-14%	-19%	-16%	-12%	-10%	-11%	-8%	-7%
H10/H11	438	453	-10%	-17%	-10%	-17%	-14%	-19%	-15%	-12%	-8%	-10%	-7%	-6%
H10/H11	438	455	-10%	-13%	-7%	-11%	-9%	-12%	-10%	-8%	-6%	-9%	-5%	*
H10/H11[#]	439	455	-15%	-14%	-9%	-12%	-13%	-16%	-12%	-9%	-5%	-7%	-6%	-5%
H10/H11[#]	439	455	-9%	-15%	-11%	-17%	-15%	-16%	-13%	-10%	-7%	-8%	-7%	-3%
H11	462	479	-12%	-17%	-9%	-16%	-11%	-18%	-11%	-12%	-6%	-10%	-6%	-5%
H12	492	497	0%	-1%	-2%	-2%	-2%	-2%	-3%	1%	-1%	-1%	-2%	-4%
H12	492	502	-1%	2%	2%	1%	1%	3%	2%	3%	0%	-1%	-2%	-3%
Ki(nM) Rα			0.16	0.20	0.37	0.09	3.00	0.34	0.65	0.67	0.44	0.21	0.32	2.60
Ki(nM) Rβ			0.19	0.25	2.74	0.08	2.80	0.48	5.10	1.47	2.40	0.28	1.30	0.30
ERβ Agonist EC50 nM; (% stim)			0.12 (100)	-	-	0.14 (97)	>10000	>10000	-	232 (104)	>10000	>10000	>10000	-
ERβ Antag IC50 (% inhib.)			NA	-	-	>10000	12 (109)	3.62 (103)	-	>10000	202 (112)	15.6 (114)	204 (108)	-

≤-20%
≤-10%
<-5%
≤5%

[a]The residue numbers of analyzed peptides relative to full-length ERβ have been tabulated. The percentage numbers listed under each compound name demonstrate the averaged differences in deuteration level of the corresponding peptide in the absence and presence of a ligand [the average calculation is based on five HDX experiments with different exchange times (1, 30, 60, 900, and 4200 s)]. We consider a change in the deuteration level of only >5% to be significant on the basis of the precision of the platform. A negative percentage represents an increase in the level of protection to exchange in that region of the receptor in the presence of ligand, which indicates the region has been protected when bound with ligand. [#]The same peptide was detected with different charge states. [*]Peptide not detected. For details of the calculation of K_i, IC_{50}, and EC_{50}, see Materials and Methods.

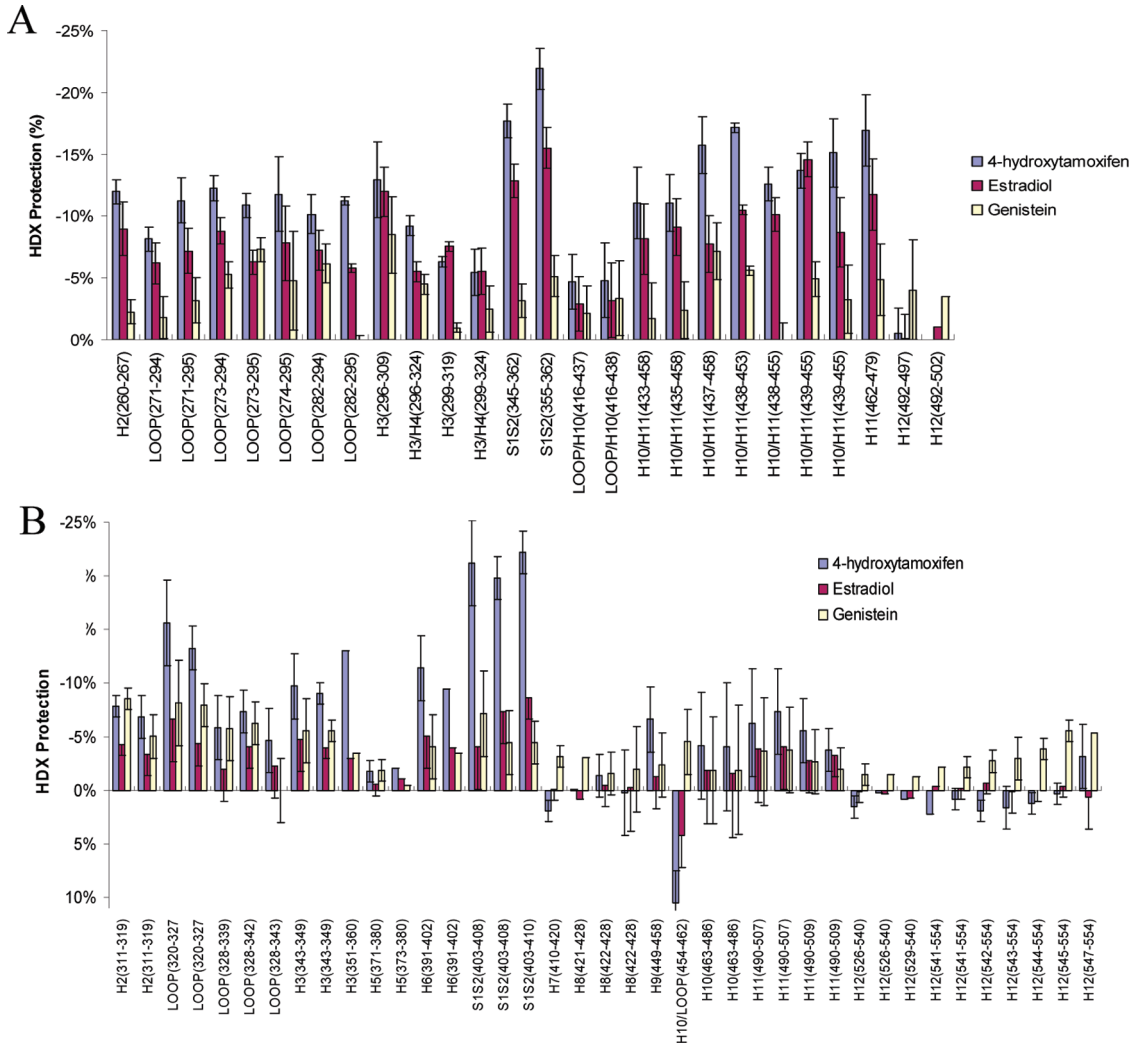

FIGURE 3: HDX analysis of ER ligands. The percentages on the *Y*-axis demonstrate the averaged differences in deuteration level of the corresponding peptide in the absence and presence of a ligand [the average calculation is based on five HDX experiments with different exchange times (1, 30, 60, 900, and 4200 s)]. (A) HDX protection (percentage) of ERβ LBD upon binding with 4-hydroxytamoxifen, E2, and genistein vs secondary structure. (B) HDX protection (percentage) of ERα LBD upon binding with 4-hydroxytamoxifen, E2, and genistein vs secondary structure. The error bars represent the standard deviation of triplicate experiments.

ICI, have divergent agonist and antagonist pharmacology in HEK293 cells. Likewise, the benzothiophenes and 17β-estradiol are clustered together on the basis of their HDX profiles but have divergent functional activity. Taken together, these data indicate that ligand-induced protection to deuterium exchange does not indicate whether a given ligand is either an agonist or an antagonist in the environment provided in these HEK cotransfection experiments. This data further support the idea that the cellular context is a critical component of functional activity. A similar observation was made for ERα in which ligand-dependent HDX protection was more predictive of cellular function in uterine cells (Ishikawa) than breast cells (MCF-7) (*20*).

DISCUSSION

Comparison of the Ligand-Induced Changes to the HDX Dynamics of ERα LBD and ERβ LBD. Under HDX conditions, only including peptide ions with a sufficient S/N in all on-exchange time points, the sequence coverage for ERβ was 60% (Table 1) whereas the sequence coverage for ERα was 66% as described in our earlier report (*20*). This difference in sequence coverage limited a direct comparison of HDX kinetics for all regions of both receptors. Fortunately, most regions of the LBD involved in ligand interaction were observed for both isoforms, including helix 2, the LOOP region between helices 2 and 3, helix 3, the β-sheet 1−β-sheet 2 region, helix 10, helix 11, and helix 12. The loop region between helix 2 and helix 3, the β-sheet 1−β-sheet 2 region, and the helix 10−helix 11 regions in ERβ LBD are among the most dynamic regions (Figure 1) and are important for the receptor−ligand interaction on the basis of the X-ray structures of both receptors (*10*, *11*). Surprisingly, the HDX kinetics of helix 12 are not altered upon ligand binding (Table 1) for either of the ER isoforms. This observation is consistent with the work of Yan et al. (*27*), who found that helix 12 in RXRα LBD has the same HDX rate in the agonist- and antagonist-bound receptor as the apoprotein. It would be expected that the HDX characteristics of the receptor reflect the context of the experiment, and changes to the dynamics of helix 12 may only be observed in the presence of coregulatory proteins, in the presence of the F domain, in the presence of DNA, or requiring the full-length receptor. However, it is important to note that in HDX studies on the LBD of PPARγ, ligand-specific changes in helix 12 dynamics were detected in the absence of both coregulatory proteins and DNA (*18*, *19*). Regardless, when the HDX behavior

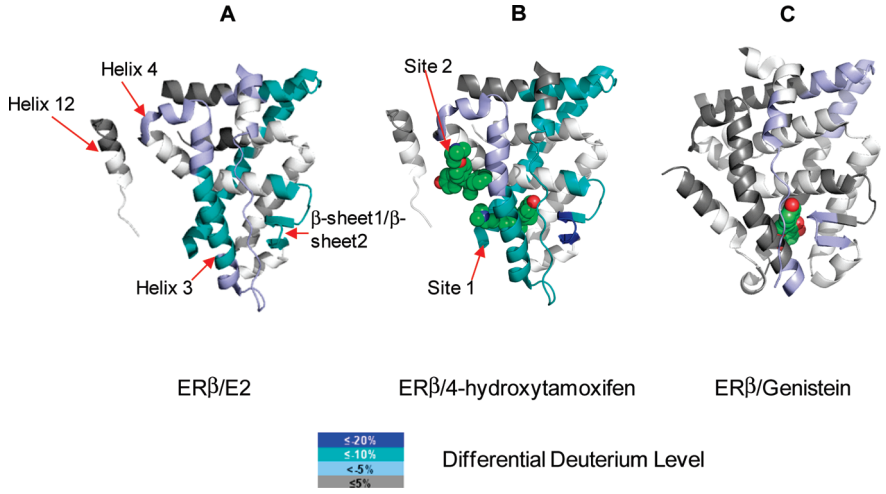

FIGURE 4: HDX profile overlaid onto ERβ LBD crystal structures. (A) HDX profile of the ERβ LBD−E2 complex overlaid onto the ERβ LBD crystal structure of 4-hydroxytamoxifen because there is no ERβ LBD−E2 X-ray data available (PDB entry 2FSZ). (B) HDX profile of the ERβ LBD−4-hydroxytamoxifen complex overlaid onto the ERβ LBD crystal structure of 4-hydroxytamoxifen (PDB entry 2FSZ). (C) HDX profile of the ERβ LBD−genistein complex overlaid on the ERβ LBD crystal structure of genistein (PDB entry 1QKM). The color legend shows the deuterium incorporation difference via subtraction of the deuterium incorporation content of holo ER from apo ER. The regions in the crystal structure that are colored white belong to peptides that are not detected after pepsin digestion or cannot be measured accurately in the HDX experiments due to co-elution problems. The ligands of 4-hydroxytamoxifen and genistein are shown as space filling diagrams.

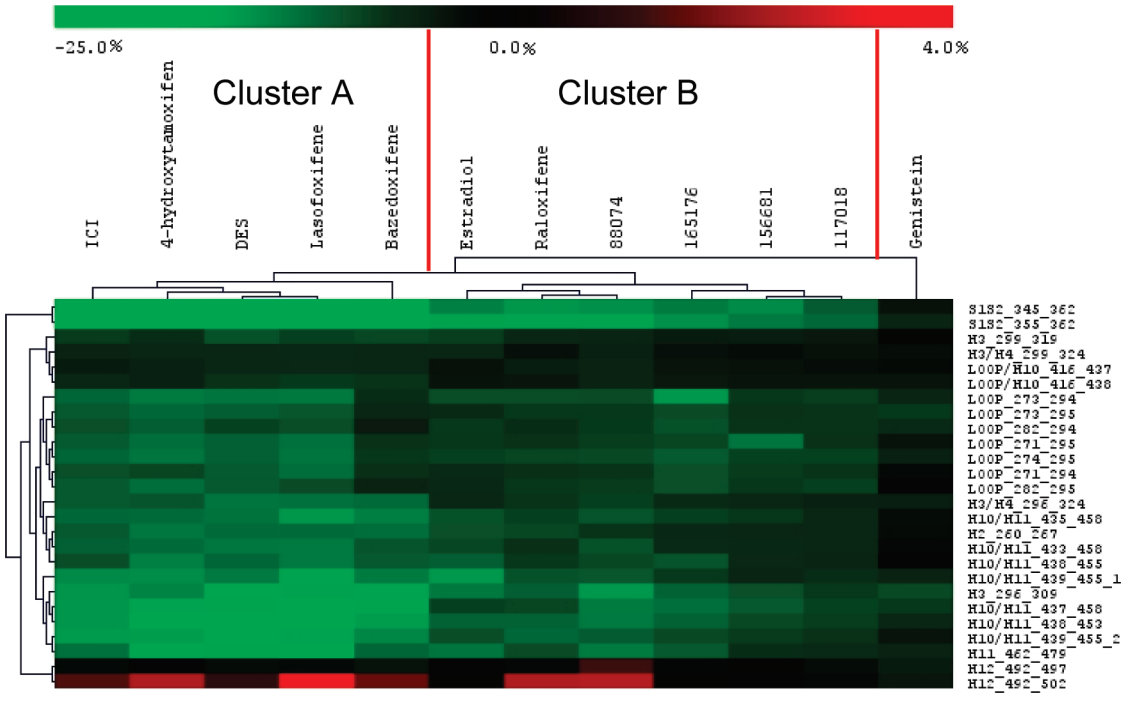

FIGURE 5: Cluster analysis of 12 ER ligands. The names of the compounds are shown at the top of the bar view, and peptide regions that have been used for cluster analysis are shown at the right of the bar view. The deuterium incorporation differences of these peptides have been treated as independent variables, and each compound has been treated as a dependent variable in the cluster analysis. The color represents the differential deuterium level of each peptide in the absence and presence of the compound. With genistein clustered as a single group, we name the other two clusters as cluster A and cluster B. Cluster A includes ICI, 4-hydroxytamoxifin, DES, lasofoxifene, and bazodoxifene. Cluster B includes estradiol, raloxifene, LY88074, LY165176, LY156681, and LY117018.

of ligands in this study is compared, the experimental context of the receptor is the same for ERα and ERβ.

Important differences were observed in the differential HDX behavior of ERβ LBD as compared to that of ERα LBD upon ligand interaction. The most acute changes occur with 17β-estradiol which significantly stabilizes ERβ LBD but has little effect on ERα LBD. Greater protection to exchange to ERβ than ERα was also observed for the ligands DES, LY88074, and ICI18278. A noteworthy observation was that compounds within the benzothiophene chemical scaffold that includes raloxifene, LY88074, LY165176, LY156681, and LY117018 demonstrate similar HDX profiles upon binding with ERβ LBD. This is very different from results obtained with ERα LBD (*20*) in which subtle structural changes within this same group of benzothiophenes resulted in distinct HDX signatures. From a structure−activity standpoint, the presence of a basic side chain appears to play little role in stabilizing ERβ LBD; i.e., the fingerprint for LY88074, which lacks this pharmacophore, is similar to those

ligands that contain a basic nitrogen (LY156681, LY165176, LY117018, and raloxifene). This is distinct from the HDX fingerprints for ERα LBD which readily distinguished those ligands, including very subtle structural differences in the positioning of this tertiary base (*20*).

The HDX kinetics of helix 3 was particularly affected. This helix, composed of amino acids 343−360 in ERα and 296−309 in ERβ, contains the aspartic acid that provides the contact point between the tertiary amine of SERMs and helix 3. For ERα, this additional contact point may play a role in stabilizing this helix relative to the apo receptor which was reflected in a protection against HDX exchange that ranges from 13% for 4-hydroxytamoxifen to < 5% for 17β-estradiol (*20*). For ERβ, such a broad range of protection was not observed; i.e., helix 3 is equivalently protected from exchange regardless of the presence or absence of a basic side chain in the ligand. For example, 17β-estradiol, which lacks this pharmacophore, provides 12% stabilization of helix 3 which is similar to the values of SERMS such as 4-hydroxytamoxifen (13% protection) and raloxifene (12% protection). Thus, the nature of the ligand plays a lesser role in ERβ than ERα in the protection of helix 3 to HDX. The reasons for this difference are not clear. When the two ER isoforms are compared, the ligand binding domains have 53% identical sequences (*1*). However, in the binding cavity, there are only two relevant amino acid substitutions, Met421 (ERα) to Ile373 (ERβ) and Leu384 (ERα) to Met336 (ERβ) (*11*, *13*). It is intriguing to speculate that the ligand-induced protection that was generally observed for helix 3 in the ERβ−ligand complex was a consequence of enhanced van der Waals interactions between helix 3 and helix 5 as a result of differential interactions between the ligand and the Leu → Met substitution on helix 5. This phenomenon has been shown to play a critical role in steroid hormone receptor function (*28*). However, more extensive work needs to be done to explore this hypothesis. Regardless, the distinct HDX dynamics we have observed between the two receptor isoforms suggest distinct receptor conformational changes that may lead to unique patterns of coregulator interaction.

Interaction of ERβ with SERMs, ER Agonists, and ER Antagonists. Cluster analysis of the HDX data for ER ligands, including SERMs, agonists, and antagonists, is presented in Figure 5. 4-Hydroxytamoxifen, lasofoxifene, and bazedoxifene cluster as one subgroup, having larger stabilization effects on ERβ LBD than raloxifene. Interestingly, raloxifene together with the other benzothiophene analogues LY88074, LY165176, LY156681, and LY117018 shares the same HDX signature, demonstrating stabilization within the loop region between helix 2 and helix 3, the β-sheet 1−β-sheet 2 region, and the H10−H11 region, suggesting that there is a unique interaction between ERβ and the sulfur-containing benzothiophene nucleus. In fact, Phe356 resides in this region of the protein, and it may interact with the polarizable sulfur in the B-ring of the benzothiophenes.

Protection to exchange between raloxifene and ERβ LBD is weaker than that observed for the ERβ LBD−4-hydroxytamoxifen complex, which is consistent with that observed in ERα LBD. A study by Wang et al. (*14*) discovered a second binding site for 4-hydroxytamoxifen in ERβ LBD which could explain the magnitude of perturbation in HDX kinetics observed in this study when the receptor is bound with 4-hydroxytamoxifen (Figure 4B). This second binding site was located within the coactivator-binding groove of ERβ LBD that involves helix 3, helix 4, helix 5, and helix 12. The second binding site could contribute to the stronger interaction in the ERβ LBD−4-hydroxytamoxifen complex if there is only one binding site in the ERβ LBD−raloxifene complex.

ERβ LBD shows significant change upon binding the agonist ligands estradiol and DES. There is greater stabilization in the ERβ LBD−agonist complex versus that of ERα LBD. It was observed in the HDX analysis of ERα LBD that most regions experience < 5% stabilization (Table 1 in ref *20*), while in ERβ LBD, most of the regions experience > 5% stabilization (Table 1). Interestingly, the same observation was obtained for the antagonist ICI 182780 where greater protection is observed when this molecule is bound to ERβ than to ERα.

Interaction of ER with Phytoestrogen Genistein. Genistein is a well-studied phytoestrogen found in soy products and reported to be protective against breast and prostate cancer (*29*). It binds both receptors with moderate affinity but has a preference for ERβ (Table 1). It was also discovered that genistein is an ERα agonist but a ERβ partial agonist (*30*) which may suggest a different regulatory mechanism for coactivator recruitment preference between the two receptors. The ERβ LBD−genistein complex has a unique HDX profile among all the compounds that have been analyzed with the least HDX protection. For example, the β-sheet 1−β-sheet 2 region was stabilized in all ERβ LBD−ligand complexes with the exception of the genistein complex. The lack of significant HDX stabilization of ERβ LBD upon binding genistein suggests little change in the conformational dynamics of the complex and is consistent with the positioning of helix 12 observed in the protein crystal structure for genistein in ERβ LBD in which the coactivator recognition site is only partially blocked by helix 12 (*11*).

CONCLUSION

In this report, we have analyzed perturbations in HDX dynamics of ERβ LBD upon binding 12 of ligands. Our results suggest ERβ has a different degree of plasticity in its LBD cavity compared with ERα. The different HDX patterns observed for ERβ LBD when compared to those of ERα LBD serve as an indication that ERβ LBD undergoes a different structural response to the same ligand when compared to ERα LBD. This further suggests distinct receptor conformational changes that may lead to unique patterns of coregulator interaction and, ultimately, tissue-selective pharmacological outcomes.

ACKNOWLEDGMENT

We are grateful for support from Mark Southern for software for analyzing the HDX data.

SUPPORTING INFORMATION AVAILABLE

Deuterium incorporation curves of representative peptides for the ERβ LBD−ligand complex showing deuterium taken up versus time (Figure S1) and comparison of the average percentages of HDX protection over five HDX time points of the ERα LBD−genistein complex to those of other ERα LBD−agonist complexes (Table S1). This material is available free of charge via the Internet at http://pubs.acs.org.

REFERENCES

1. Pearce, S. T., and Jordan, V. C. (2004) The biological role of estrogen receptors α and β in cancer. *Crit. Rev. Oncol. Hematol. 50*, 3–22.
2. Koehler, K. F., Helguero, L. A., Haldosen, L. A., Warner, M., and Gustafsson, J. A. (2005) Reflections on the discovery and significance of estrogen receptor β. *Endocr. Rev. 26*, 465–478.

3. Zhao, L., O'Neill, K., and Diaz Brinton, R. (2005) Selective estrogen receptor modulators (SERMs) for the brain: Current status and remaining challenges for developing NeuroSERMs. *Brain Res. Brain Res. Rev. 49*, 472–493.
4. Harris, H. A., Albert, L. M., Leathurby, Y., Malamas, M. S., Mewshaw, R. E., Miller, C. P., Kharode, Y. P., Marzolf, J., Komm, B. S., Winneker, R. C., Frail, D. E., Henderson, R. A., Zhu, Y., and Keith, J. C., Jr. (2003) Evaluation of an estrogen receptor-β agonist in animal models of human disease. *Endocrinology 144*, 4241–4249.
5. Couse, J. F., Lindzey, J., Grandien, K., Gustafsson, J. A., and Korach, K. S. (1997) Tissue distribution and quantitative analysis of estrogen receptor-α (ERα) and estrogen receptor-β (ERβ) messenger ribonucleic acid in the wild-type and ERα-knockout mouse. *Endocrinology 138*, 4613–4621.
6. Neubauer, B. L., McNulty, A. M., Chedid, M., Chen, K., Goode, R. L., Johnson, M. A., Jones, C. D., Krishnan, V., Lynch, R., Osborne, H. E., and Graff, J. R. (2003) The selective estrogen receptor modulator trioxifene (LY133314) inhibits metastasis and extends survival in the PAIII rat prostatic carcinoma model. *Cancer Res. 63*, 6056–6062.
7. Ali, S. H., O'Donnell, A. L., Balu, D., Pohl, M. B., Seyler, M. J., Mohamed, S., Mousa, S., and Dandona, P. (2000) Estrogen receptor-α in the inhibition of cancer growth and angiogenesis. *Cancer Res. 60*, 7094–7098.
8. Harris, H. A. (2007) Estrogen receptor-β: Recent lessons from in vivo studies. *Mol. Endocrinol. 21*, 1–13.
9. Imamov, O., Shim, G. J., Warner, M., and Gustafsson, J. A. (2005) Estrogen receptor β in health and disease. *Biol. Reprod. 73*, 866–871.
10. Brzozowski, A. M., Pike, A. C., Dauter, Z., Hubbard, R. E., Bonn, T., Engstrom, O., Ohman, L., Greene, G. L., Gustafsson, J. A., and Carlquist, M. (1997) Molecular basis of agonism and antagonism in the oestrogen receptor. *Nature 389*, 753–758.
11. Pike, A. C., Brzozowski, A. M., Hubbard, R. E., Bonn, T., Thorsell, A. G., Engstrom, O., Ljunggren, J., Gustafsson, J. A., and Carlquist, M. (1999) Structure of the ligand-binding domain of oestrogen receptor β in the presence of a partial agonist and a full antagonist. *EMBO J. 18*, 4608–4618.
12. Shiau, A. K., Barstad, D., Loria, P. M., Cheng, L., Kushner, P. J., Agard, D. A., and Greene, G. L. (1998) The structural basis of estrogen receptor/coactivator recognition and the antagonism of this interaction by tamoxifen. *Cell 95*, 927–937.
13. van Hoorn, W. P. (2002) Identification of a second binding site in the estrogen receptor. *J. Med. Chem. 45*, 584–589.
14. Wang, Y., Chirgadze, N. Y., Briggs, S. L., Khan, S., Jensen, E. V., and Burris, T. P. (2006) A second binding site for hydroxytamoxifen within the coactivator-binding groove of estrogen receptor β. *Proc. Natl. Acad. Sci. U.S.A. 103*, 9908–9911.
15. Yan, X., Broderick, D., Leid, M. E., Schimerlik, M. I., and Deinzer, M. L. (2004) Dynamics and ligand-induced solvent accessibility changes in human retinoid X receptor homodimer determined by hydrogen deuterium exchange and mass spectrometry. *Biochemistry 43*, 909–917.
16. Yan, X., Deinzer, M. L., Schimerlik, M. I., Broderick, D., Leid, M. E., and Dawson, M. I. (2006) Investigation of ligand interactions with human RXRα by hydrogen/deuterium exchange and mass spectrometry. *J. Am. Soc. Mass Spectrom. 17*, 1510–1517.
17. Chalmers, M. J., Busby, S. A., Pascal, B. D., He, Y., Hendrickson, C. L., Marshall, A. G., and Griffin, P. R. (2006) Probing protein ligand interactions by automated hydrogen/deuterium exchange mass spectrometry. *Anal. Chem. 78*, 1005–1014.
18. Hamuro, Y., Coales, S. J., Morrow, J. A., Molnar, K. S., Tuske, S. J., Southern, M. R., and Griffin, P. R. (2006) Hydrogen/deuterium-exchange (H/D-Ex) of PPARγ LBD in the presence of various modulators. *Protein Sci. 15*, 1883–1892.
19. Bruning, J. B., Chalmers, J. M., Prasad, D., Busby, S. A., Kamenecka, K. M., He, Y., Nettles, K. M., and Griffin, P. R. (2007) Partial Agonists Activate PPARg Using a Helix 12 Independent Mechanism. *Structure 15*, 1258–1271.
20. Dai, S. Y., Chalmers, M. J., Bruning, J., Bramlett, K. S., Osborne, H. E., Montrose-Rafizadeh, C., Barr, R. J., Wang, Y., Wang, M., Burris, P. T., Dodge, J. A., and Griffin, P. R. (2007) Prediction of the Tissue-Specificity of Selective Estrogen Receptor Modulators using a Single Biochemical Method. *Proc. Natl. Acad. Sci. U.S.A. 105*, 7171–7176.
21. Kuiper, G. G., Carlsson, B., Grandien, K., Enmark, E., Haggblad, J., Nilsson, S., and Gustafsson, J. A. (1997) Comparison of the ligand binding specificity and transcript tissue distribution of estrogen receptors α and β. *Endocrinology 138*, 863–870.
22. Chalmers, M. J., Busby, S. A., Pascal, B. D., Southern, M. R., and Griffin, P. R. (2007) A two-stage differential hydrogen deuterium exchange method for the rapid characterization of protein/ligand interactions. *J. Biomol. Tech. 18*, 194–204.
23. Pascal, B. D., Chalmers, M. J., Busby, S. A., Mader, C. C., Southern, M. R., Tsinoremas, N. F., and Griffin, P. R. (2007) The Deuterator: Software for the determination of backbone amide deuterium levels from H/D exchange MS data. *BMC Bioinf. 8*, 156.
24. Bai, Y., Milne, J. S., Mayne, L., and Englander, S. W. (1993) Primary structure effects on peptide group hydrogen exchange. *Proteins 17*, 75–86.
25. Englander, S. W. (2006) Hydrogen exchange and mass spectrometry: A historical perspective. *J. Am. Soc. Mass Spectrom. 17*, 1481–1489.
26. Saeed, A. I., Sharov, V., White, J., Li, J., Liang, W., Bhagabati, N., Braisted, J., Klapa, M., Currier, T., Thiagarajan, M., Sturn, A., Snuffin, M., Rezantsev, A., Popov, D., Ryltsov, A., Kostukovich, E., Borisovsky, I., Liu, Z., Vinsavich, A., Trush, V., and Quackenbush, J. (2003) TM4: A free, open-source system for microarray data management and analysis. *BioTechniques 34*, 374–378.
27. Yan, X., Perez, E., Leid, M., Schimerlik, M. I., de Lera, A. R., and Deinzer, M. L. (2007) Deuterium exchange and mass spectrometry reveal the interaction differences of two synthetic modulators of RXRα LBD. *Protein Sci. 16*, 2491–2501.
28. Zhang, J., Simisky, J., Tsai, F. T., and Geller, D. S. (2005) A critical role of helix 3-helix 5 interaction in steroid hormone receptor function. *Proc. Natl. Acad. Sci. U.S.A. 102*, 2707–2712.
29. Adlercreutz, H., and Mazur, W. (1997) Phyto-oestrogens and Western diseases. *Ann. Med. 29*, 95–120.
30. Barkhem, T., Carlsson, B., Nilsson, Y., Enmark, E., Gustafsson, J., and Nilsson, S. (1998) Differential response of estrogen receptor α and estrogen receptor β to partial estrogen agonists/antagonists. *Mol. Pharmacol. 54*, 105–112.